© 2023 Journal of Pharmacy & Pharmacognosy Research, 11 (6), 1056-1071, 2023
ISSN 0719-4250
https://jppres.com

DOI: https://doi.org/10.56499/jppres23.1727_11.6.1056

*Original Article*

# Natural deep eutectic solvent extraction of xanthorrhizol and curcuminoids from *Curcuma xanthorrhiza* Roxb and simultaneous determination by high-performance liquid chromatography

[Extracción natural con disolvente eutéctico profundo de xantorrhizol y curcuminoides de *Curcuma xanthorrhiza* Roxb y determinación simultánea mediante cromatografía líquida de alta resolución]

**Adelina Simamora[1,2,3], Kris H. Timotius[2], Heri Setiawan[3,4], Masteria Y. Putra[3,5], Abdul Mun'im[3,6*]**

[1]Graduate Program in Pharmaceutical Sciences, Faculty of Pharmacy, Universitas Indonesia, 16424, Depok, Indonesia.
[2]Department of Biochemistry, Faculty of Medicine and Health Sciences, Krida Wacana Christian University, 11510, Jakarta, Indonesia.
[3]National Metabolomics Collaborative Research Center, Faculty of Pharmacy, Universitas Indonesia, 16424, Depok, West Java, Indonesia.
[4]Department of Pharmacology, Faculty of Pharmacy, Universitas Indonesia, 16424, Depok, Indonesia.
[5]Research Center for Vaccine and Drug, Research Organization for Health, National Research and Innovation Agency (BRIN), 16911, Cibinong, West Java, Indonesia.
[6]Department of Pharmacognosy-Phytochemistry, Faculty of Pharmacy, Universitas Indonesia, 16424, Depok, Indonesia.
*E-mail: munim@farmasi.ui.ac.id

## Abstract

*Context*: *Curcuma xanthorrhiza*, a native to Indonesia, has been recognized as a potential medicinal plant. Xanthorrhizol (XTZ), curcumin (Cur), bisdemethoxycurcumin (BDMC), and demethoxycurcumin (DMC) are the main major metabolites with different bioactivities. Thus, the selective extraction of these markers is required.

*Aims*: To characterize and use natural deep eutectic solvents (NADES) for the extraction of XTZ and curcuminoids (CURS) from *C. xanthorrhiza*.

*Methods*: Four NADES, comprising of glucose:lactic acid (Glu:LA, 1:3), choline chloride: malic acid (ChCl:MA, 1:1), choline chloride: glycerol (ChCl:Gly, 1:1), and choline chloride: sucrose (ChCl:Suc, 3:1) were synthesized and subjected to FTIR. The physicochemical properties of NADES were characterized, including polarity, viscosity, and density. Their antioxidant profiles were evaluated. The toxicity of NADES was assessed towards *Escherichia coli* by real-time growth monitoring. Tested NADES were employed to extract marker compounds from the rhizome of *C. xanthorrhiza.* A validated high-performance liquid chromatography (HPLC) method was applied to simultaneously quantify XTZ and CURS in NADES extracts.

*Results*: FTIR spectra confirmed the formation of hydrogen bonds between components. Using the DPPH and FRAP methods, all NADES and NADES extracts displayed antioxidative activity, suggesting the contribution of NADES to the activity. Of the tested NADES, Glu:LA (1:3) obtained the highest content of XTZ over Cur, BDMC, and DMC, comparable to that of ethanol maceration. All tested NADES were harmless to *E. coli*, except for ChCl:MA (1:1). However, NADES extracts of Glu:LA (1:3) and ChCl:MA (1:1) suppressed the growth of the bacterium. Scanning electron micrographs demonstrated the destruction of the surface structure of the rhizome powder by NADES-ultrasonication.

*Conclusions*: The study recommended the use of Glu:LA (1:3) to selectively extract XTZ to promote environmentally friendly and sustainable extraction.

*Keywords*: *Escherichia coli*; scanning electron microscopy; terpenoid; toxicity test; viscosity.

## Resumen

*Contexto*: La *Curcuma xanthorrhiza*, originaria de Indonesia, ha sido reconocida como una planta medicinal potencial. Xanthorrhizol (XTZ), curcumin (Cur), bisdemethoxycurcumin (BDMC), and demethoxycurcumin (DMC) are the main major metabolites with different bioactivities. Por lo tanto, se requiere la extracción selectiva de estos marcadores.

*Objetivos*: Caracterizar y utilizar disolventes eutécticos profundos naturales (NADES) para la extracción de XTZ y curcuminoides (CURS) de *C. xanthorrhiza*.

*Métodos:* Se sintetizaron cuatro NADES, compuestos de glucosa:ácido láctico (Glu:LA, 1:3), cloruro de colina: ácido málico (ChCl:MA, 1:1), cloruro de colina: glicerol (ChCl:Gly, 1:1), y cloruro de colina: sacarosa (ChCl:Suc, 3:1) y se sometieron a FTIR. Se caracterizaron las propiedades fisicoquímicas de los NADES, como la polaridad, la viscosidad y la densidad. Se evaluaron sus perfiles antioxidantes. Se evaluó la toxicidad de los NADES frente a *Escherichia coli* mediante la monitorización del crecimiento en tiempo real. Los NADES probados se emplearon para extraer compuestos marcadores del rizoma de *C. xanthorrhiza*. Se aplicó un método validado de cromatografía líquida de alta resolución (HPLC) para cuantificar simultáneamente XTZ y CURS en extractos de NADES.

*Resultados*: Los espectros FTIR confirmaron la formación de enlaces de hidrógeno entre los componentes. Mediante los métodos DPPH y FRAP, todos los extractos de NADES y NADES mostraron actividad antioxidante, lo que sugiere la contribución de los NADES a la actividad. De los NADES ensayados, Glu:LA (1:3) obtuvo el mayor contenido de XTZ sobre Cur, BDMC y DMC, comparable al de la maceración con etanol. Todos los NADES ensayados fueron inocuos para E. coli, excepto ChCl:MA (1:1). Sin embargo, los extractos NADES de Glu:LA (1:3) y ChCl:MA (1:1) suprimieron el crecimiento de la bacteria. Las micrografías electrónicas de barrido demostraron la destrucción de la estructura superficial del polvo de rizoma por la ultrasonicación con NADES.

*Conclusiones*: El estudio recomendó el uso de Glu:LA (1:3) para extraer selectivamente XTZ con el fin de promover una extracción respetuosa con el medio ambiente y sostenible.

*Palabras Clave*: ensayo de toxicidad; *Escherichia coli*; microscopía electrónica de barrido; terpenoide; viscosidad.

ARTICLE INFO
Received: June 19, 2023.
Accepted: September 27, 2023.
Available Online: October 4, 2023.

AUTHOR INFO
ORCID:
0000-0002-7337-093X (AS)
0000-0001-7232-0001 (KHT)
0000-0002-0170-9885 (HS)
0000-0002-9879-3293 (MYP)
0000-0002-6681-9196 (AM)

**Abbreviations:** AAE: Ascorbic acid equivalent; BDMC: Bisdemethoxycurcumin; Cur: Curcumin; CURS: Curcuminoids; DES: Deep eutectic solvents; DMC: Demethoxycurcumin; DPPH: 2,2-diphenyl-1-picrylhydrazyl; ChCl:Gly: Choline chloride:glycerol; ChCl:MA: Choline chloride:malic acid; ChCl:Suc: Choline chloride:sucrose; FRAP: Ferric-reducing antioxidant power; Glu:LA: Glucose:lactic acid; HBA: Hydrogen bond acceptor; HBD: Hydrogen bond donor; NADES: Natural deep eutectic solvents; TE: Trolox equivalent; TPTZ: 2,4,6- tris(2-pyridyl)-s-triazine; SEM: Scanning electron microscopy; XTZ: Xanthorrhizol.

## INTRODUCTION

*Curcuma xanthorrhiza,* which belongs to the family *Zingiberaceae*, is a valuable medicinal plant that originates from Indonesia. *C. xanthorrhiza* is a ubiquitous constituent of Indonesian traditional health formulations (known as jamu). It originates from Indonesia, where it is commonly known as Temulawak or Java turmeric. Traditionally, rhizomes have been used as a health supplement and for the treatment of stomach and liver disorders such as constipation, diarrhea, and jaundice (Hirschhorn, 1983; Hwang et al., 2000). Studies reported different bioactivities of *C. xanthorrhiza*, including antimicrobial, antioxidant, antinociceptive, anti-inflammatory, and hepatoprotective activities (Devaraj et al., 2010; 2014; Hwang et al., 2000; Mary et al., 2012). The health benefits of *C. xanthorrhiza* are due to its major metabolites—i.e., xanthorrhizol (XTZ), curcumin (Cur), bisdemethoxycurcumin (BDMC), demethoxycurcumin (DMC). XTZ is found in significant abundance in *C. xanthorrhiza* (Mary et al., 2012); thus, it is an important marker that distinguishes this plant from other Curcuma species (Nurcholis et al., 2018).

Literature has confirmed various pharmacological activities of XTZ, such as anticancer, antioxidant, anti-inflammatory, antimicrobial, and protective effects on important organs (He et al., 2015; Oon et al., 2015; Sahebkar et al., 2015; Simamora et al., 2022). Conventional extraction of XTZ from *C. xanthorrhiza* rhizomes mostly depends on organic solvents (Nurcholis et al., 2018), which are volatile, flammable, non-biodegradable, and, thus, toxic to human health and the environment. Natural deep eutectic solvents (NADES) have been gaining attention as a green alternative to organic solvents due to their beneficial physicochemical properties such as low vapor pressure, non-flammability, high thermal stability, and polarity (Rente et al., 2021). NADES are composed of hydrogen bond acceptor and hydrogen bond donor components that exist in different types of cells and organisms. Therefore, NADES are considered biodegradable and safer than organic solvents (Radošević et al., 2015). Studies reported that the use of NADES as an extractant increased the bioactivities of plant metabolites, such as antioxidants (Bakirtzi et al., 2016), antimicrobial (Grozdanova et al., 2020), and inhibition activities on enzymes involved in pathological conditions (Ahmad et al., 2020; Oktaviyanti et al., 2019). Recently, choline chloride- and glucose-based NADES have been developed for the extraction of curcuminoids from *C. longa* and showed comparable extraction efficiency to organic solvent extraction (Liu et al., 2019; Patil et al., 2021). However, to date, no study has reported the use of NADES for the extraction of XTZ from *C. xanthorrhiza.*

In this study, four choline chloride- and glucose-based NADES (Fig. 1) were evaluated as extractants for XTZ from the rhizome of *C. xanthorrhiza*. The physicochemical characterization of NADES under study was described. NADES extracts were analyzed simultaneously by high-performance liquid chromatography (HPLC) for XTZ, Cur, BDMC, and DMC contents. Further, NADES were evaluated for their antioxidant activity and toxicity profile toward *Escherichia coli*. Surface morphology was undertaken to investigate the effect of NADES on extraction.

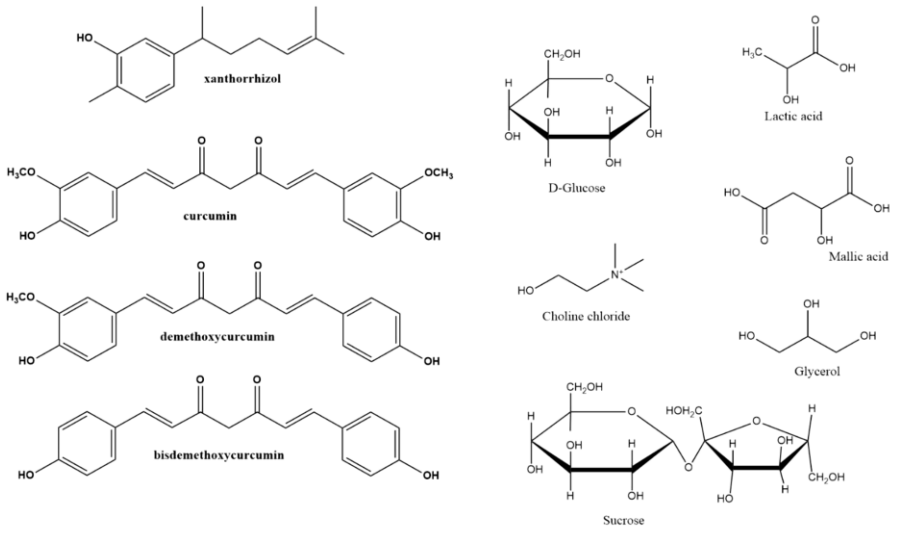



**Figure 1.** Marker compounds from *Curcuma xanthorrhiza* and NADES components under study.

**Table 1.** NADES prepared in this study and their abbreviations.

| NADES components | | HBD:HBA (ratio) | Sample name | Water content (%, v/v) | S/L ratio (g/mL)* | Duration of sonication (min) | Liquid appearance |
|---|---|---|---|---|---|---|---|
| HBA | HBD | | | | | | |
| Glucose | Lactic acid | 1:3 | Glu:LA (1:3) | 30 | 1/15 | 20 | Slightly viscous, transparent |
| Choline chloride | Malic acid | 1:1 | ChCl:MA (1:1) | 25 | 1/15 | 15 | Moderately viscous, transparent |
| Choline chloride | Glycerol | 1:1 | ChCl:Gly (1:1) | 10 | 1/25 | 20 | Slightly viscous, transparent |
| Choline chloride | Sucrose | 3:1 | ChCl:Suc (3:1) | 10 | 1/25 | 20 | Highly viscous, transparent |

*One gram of rhizome powder was used for each extraction. HBD: hydrogen bond donor; HBA: hydrogen bond acceptor.

## MATERIAL AND METHODS

### Reagents

Choline chloride (ChCl) was purchased from Xi'an Rongsheng Biotechnology (Xi'an, China). D-glucose (Glu) and sucrose were obtained from Merck (Darmstadt, Germany). 2,2-diphenyl-1-picrylhydrazyl (DPPH), **g**lycerol (87%), **l**actic acid (≥85%), DL-malic acid (≥99%), Nile red, and 2,4,6- tris(2-pyridyl)-s-triazine (TPTZ) were obtained from Sigma Aldrich (St. Louis, MO, USA). Curcumin (Cur) was obtained from Fitopure (Pandang, Indonesia), bisdemethoxycurcumin (BDMC), demethoxycurcumin (DCM), and xanthorrhizol (XTZ) were bought from MarkHerb (Bandung, Indonesia). The standard compounds had a purity of >95%. HPLC-grade acetonitrile, methanol, and formic acid were purchased from SmartLab (Tangerang, Indonesia). Bidistilled water pro injection was obtained from IkaPharmindo Putramas (Jakarta, Indonesia).

### NADES preparation

Four types of NADES were prepared, with components as described in Table 1. The chemical structures of NADES components are shown in Fig. 1. The selection of these NADES, including the molar ratios of the starting components, was based on preliminary screening as described in (Amartya, 2022; Kusumowardhani, 2022; Nadia, 2022; Putri, 2022). NADES components—i.e., hydrogen bond acceptor (HBA) and hydrogen bond donor (HBD) —were mixed in a predetermined molar ratio and continuously stirred at 70°C at 300 rpm agitation speed until a clear and homogenous liquid was formed (Duan et al., 2016). Each NADES contained different percentages of water (Putri, 2022) to help reduce the viscosity.

### Physicochemical properties of NADES

The viscosities of NADES were measured using a Brookfield DVPlus viscometer (Middleboro, USA) (Mulia et al., 2015). Measurement was carried out using a CP-41 spindle running at a specific speed in the full-scale range. The viscosity accuracy was ± 1.0 % using this spindle.

The densities of NADES were determined using an Isolab pycnometer (Eschau, Germany) (Santana et al., 2019b). The density accuracy was ± 0.001 g/cm$^3$. Measurement was performed at 25°C.

The polarity of prepared NADES was determined using Nile red as a solvatochromic probe, as described previously (Ogihara et al., 2004). Polarity was determined by measuring the $\lambda_{max}$ shift of Nile red (9-diethylamino-5-benzo[a]phenoxazinone) in NADES. A Nile red stock solution was prepared in ethanol (1 g/L) and stored at 4°C. The stock solution was diluted 100 times with ethanol and added to each NADES. Maximum absorbance in the visible region (400-750 nm) was measured by a spectrophotometer using a 1 cm quartz cell. The molar transition energy was calculated using the following formula [1] (Reichardt, 1994).

$$E_{NR}\ (kcal/mol) = 28.591 / \lambda_{max} \quad [1]$$

### Plant material

Fresh rhizomes of *C. xanthorrhiza* were obtained from Balittro (Research Institute for Herbs and Spices) Bogor, Indonesia (-6.576893345305293, 106.78633149414519). The plant was identified by the Centre for Biosystematics Research and Evolution (Pusat Riset Biosistematika dan Evolusi), Herbarium Bogoriense, Bogor, Indonesia (voucher number: B-609/V/DI.05.07/3/2022). Rhizomes were thinly

sliced and dried at 40°C with a food dehydrator for several days. Dried rhizomes were pulverized using a mechanical grinder, and the powder was sieved through 60 mesh sieves. The dried rhizome powder was stored at 4°C before use for extraction.

**NADES extraction**

NADES extractions of *C. xanthorriza* rhizome were conducted following extraction conditions as reported previously (Putri, 2022), including the solid-to-liquid ratio and sonication duration (Table 1). After sonication (40 kHz) (Bandelin Sonorex Digitec, Berlin, Germany), the extract was centrifuged at 7000 rpm for 10 mins in a laboratory centrifuge. The supernatant was separated by filtration using a Whatman No. 1 filter paper, protected from light, and kept at room temperature until further use.

Extraction by conventional solvents was carried out for comparison. By virtue of its biological activities, *C. xanthorrhiza* has been listed in the Indonesian Herbal Pharmacopeia. As recommended by the Indonesian Herbal Pharmacopeia, ethanol maceration is used for the extraction of *C. xanthorrhiza* (Kementerian Kesehatan, 2017). Dried pulverized rhizomes of *C. xanthorrhiza* were macerated in ethanol 96% (1:10). After 24 h, the supernatant was separated by filtration, and the macerate was re-macerated with half the volume used in the previous maceration. All filtrates were then pooled and evaporated under reduced pressure using a Buchi rotary vacuum evaporator (Flawil, Switzerland) to obtain dried crude extract.

**HPLC-UV analysis of NADES extracts**

*Chromatography instrumentation*

Chromatography was conducted using a Schambeck HPLC system (Schambeck SFD GmbH, Bad Honnef, Germany) equipped with S 9425 HPLC pumps, an S 8515 vacuum degasser, and an S 4245 UV-Vis detector. Data acquisition and processing were performed using Clarity software by DataApex (Prague, Czech Republic).

*Chromatographic conditions*

Chromatographic analyses for XTZ, Cur, BDMC, and DMC were conducted based on a method of Erpina et al. (2017) with some modifications. A Zodiac C18 column (150 mm × 4.6 mm, 5 µm) (Zodiac Life Sciences, Hyderabad, India) was used for chromatographic separation. The mobile phase consisted of acetonitrile (eluent A) and formic acid 0.07% in water (eluent B) with a gradient mode of elution, with conditions as follows: 0-5 min, 45-50% A; 5-10 min, 50-55% A; 10-25 min, 55-60% A, 25-35 min, 60-65% A, 35-45 min, 65-70% A, 45-60 min, 70-100% A and 60-65 min 100% A. Samples (20 µL) were loaded and eluted at a flow rate of 0.6 mL/min at room temperature. XTZ was read at 275 nm, whereas BDMC, DMC, and Cur were identified at 425 nm.

*Standard solutions, method validation, and analysis*

Stock solutions of XTZ, Cur, BDMC, and DMC were prepared in methanol by accurately weighing each standard compound to make concentrations of 1000 µg/mL. Working standard solutions were prepared by dilution of precise amounts of the stock solution with methanol to make seven concentration points of 5-400 µg/mL for XTZ, whereas for BDMC, DMC, and Cur were in the range of 2.5-100 µg/mL. To allow simultaneous determination, prepared standard solutions of XTZ, Cur, BDMC, and DMC at certain concentrations were mixed at a 1:1:1:1 ratio to make calibrator solutions. All calibrators were filtered through a 0.45 µm nylon filter prior to injection. Areas under the curves for each standard were recorded and plotted against their corresponding concentrations to generate calibration curves of XTZ, Cur, BDMC, and DMC.

Validation of the analysis method was carried out according to the Association of Analytical Communities (AOAC) (AOAC, 2012). Table 2 shows the validation of the linearity of calibration curves, accuracy and precision, the limit of detection, and the limit of quantification. Quantification for each marker compound in NADES extracts was performed using the validated method at the wavelength maxima for each compound.

HPLC analysis was performed for NADES and ethanol extracts by diluting 1 mL of each crude extract in methanol in a 5 mL volumetric flask. The solution was then syringe-filtered by a 0.45 µm nylon membrane prior to injection.

*Fourier transform infrared (FTIR) analysis*

The IR spectra of NADES and their starting components were obtained by an Agilent Cary 630 FTIR spectrophotometer (Santa Clara, USA). Samples were scanned in an attenuated total reflectance (ATR) mode in the range of 4000-650 $cm^{-1}$, with a resolution of 4 $cm^{-1}$ and an accumulation of 16 scans.

*Scanning electron microscopy analysis*

The surface morphology images of the rhizome powder (*C. xanthorrhiza*) were obtained using Jeol JSM IT200 SEM equipment. Samples were dried and coated with a thin layer of gold. A 20 kV accelerating voltage was applied for measurement.

**Table 2.** Regression analysis, the limit of detection (LOD), and the limit of quantification (LOQ) of the quantitative determination of XTZ, Cur, BDMC, and DMC.

| Standard compounds[a] | Retention time | Regression equations (y = ax + b) | Correlation coefficient ($R^2$) | LOD (µg/mL) | LOQ (µg/mL) |
|---|---|---|---|---|---|
| XTZ | 44.37 ± 0.48 | y = 4.42x + 9.0517 | 0.9989 | 15.84 | 52.80 |
| Cur | 14.20 ± 0.85 | y = 44.233x - 28.563 | 0.9995 | 4.42 | 14.73 |
| BDMC | 12.45 ± 0.85 | y = 43.308x - 66.297 | 0.9982 | 5.48 | 18.27 |
| DMC | 13.30 ± 0.70 | y = 64.041x - 67.529 | 0.9972 | 6.73 | 22.42 |

[a]XTZ: xanthorrhizol; Cur: curcumin; BDMC: bisdemethoxycurcumin; and DMC: demethoxycurcumin. [b]Concentration range for Cur, BDMC, and DMC was 2.5-100 µg/mL, and for XTZ was 5-400 µg/mL.

### Antioxidant assays

*Ferric-reducing antioxidant power (FRAP) assay*

The antioxidant profile of NADES and NADES extracts was measured using the ferric-reducing antioxidant power (FRAP) assay, as reported previously (Bolanos de la Torre et al., 2015). In brief, an aliquot of each sample (20 µL) was put into a 96-well microplate, then was followed by the addition of FRAP reagent (280 uL). The mixture was incubated in the dark at 37°C and shaken at 300 RPM for 30 mins at 37°C on a Thermostar BMG Labtech microplate shaker/incubator (Ortenberg, Germany). The absorbance was recorded at 595 nm using an iMark BioRad microplate reader (Hercules, USA). FRAP reagent was prepared by mixing 2,4,6-tripyridyl-*s*-triazine salt (TPTZ) (10 mM in HCl 40 mM), $FeCl_2$ (20 mM), and acetate buffer (300 mM, pH 3.6) in 1:1:10 ratio. The experiments were conducted in four replicates. A standard curve was generated using trolox (50-800 µmol/mL), which obtained y = 0.0021x + 0.1493 ($R^2$ = 0.999). FRAP activity was expressed as µmol Trolox equivalent/gram (µmol TE/g) NADES.

*DPPH radical scavenging assay*

The ability of NADES and NADES extracts to scavenge DPPH radicals was evaluated by the method described by Hilma et al. (2019). An aliquot of each sample (50 µL) was put into a 96-well microplate. Each sample was then mixed with a DPPH solution (80 µL, 0.6 mM in methanol). The solution was shaken in the dark using a Thermostar BMG Labtech microplate shaker/incubator at 300 rpm for 30 mins at 25°C. The absorbance was read at 515 nm using an iMark BioRad microplate reader (Hercules, California, USA). The experiments were conducted in four replicates. A standard curve was prepared using ascorbic acid as a standard antioxidant agent, which obtained a regression equation of y = -1.4887x + 0.9992 ($R^2$ = 0.9729). The results were presented as µmol ascorbic acid equivalent (AAE)/g NADES or dried rhizome for extracts.

### Bacterial toxicity assay

The toxicity profiles of NADES and NADES extracts were evaluated by monitoring real-time bacterial growth on *E. coli*, as described previously (Torregrosa-Crespo et al., 2020), with some modifications. The inoculum of *E. coli* ATCC 35218 was prepared by growing pre-inoculum cells in the Luria-Bertani media under constant shaking at 37°C for 20 h. For the toxicity experiment, the reaction mixture was prepared as follows. Aliquots of 15 mL of Luria-Bertani medium (LB), *E. coli* inoculum (500 µL), and NADES (50 µL) were added into a corning tube. The tube was then placed in a bioreactor (BioSan RTS 001/001C, Latvia). The cells were grown at 37°C with a constant rotation speed (500 rpm). The growth of the bacterium was monitored using the bioreactor by reading the optical density (OD) at 850 nm every 15 min for 20 h. The experiments were conducted in two replicates.

### Statistical analysis

Experiments were performed in three repeats, and results were presented as mean ± standard deviation (SD). Analysis of significant differences was conducted using a Student's *t*-test and a one-way ANOVA (post hoc with Tuckey test), with $p<0.05$ considered statistically significant.

## RESULTS AND DISCUSSION

Within the present work, four types of NADES were prepared using the heating and stirring methods. All NADES turned into an eutectic mixture at 70°C after continuous stirring for 10 to 30 min. Each NADES is a homogenous liquid with no precipitation and remains in one phase for more than three months at ambient temperature.

### Characterization of NADES

The physicochemical properties, including polarity, viscosity, density, pH, and the antioxidant profiles

**Table 3.** Physicochemical characterization of NADES systems.

| Sample name | Polarity (kcal/mol)* | Viscosity (CPS)** | Density (g/cm)* | pH* |
|---|---|---|---|---|
| Glu:LA (1:3) | 47.91 ± 0.24$^{cde}$ | 30.43 ± 0.15$^{b}$ | 1.26 ± 0.01$^{ce}$ | 1.83 ± 0.13$^{bcd}$ |
| ChCl:MA (1:1) | 47.76 ± 0.05$^{cde}$ | 68.03 ± 0.47$^{ac}$ | 1.25 ± 0.03$^{ce}$ | 0.32 ± 0.03$^{acd}$ |
| ChCl:Gly (1:1) | 49.99 ± 0.48$^{abe}$ | 31.13 ± 0.55$^{b}$ | 1.16 ± 0.01$^{abde}$ | 6.19 ± 0.05$^{abd}$ |
| ChCl:Suc (3:1) | 49.89 ± 0.45$^{abe}$ | NA‡ | 1.27 ± 0.01$^{ce}$ | 5.75 ± 0.07$^{abc}$ |
| Ethanol | 51.82 ± 0.39$^{abcd}$ | ND§ | 0.79 ± 0.01$^{abcd}$ | NA‡ |

*Polarity, density, and pH were determined from two independent measurements and expressed as mean ± SD. Different letters indicate statistically significant differences with Tukey analysis ($p<0.05$). **Viscosity was determined from three independent measurements and expressed as mean ± SD. ‡NA (not applicable, viscosity >49.152 CPS. §ND (not determined).

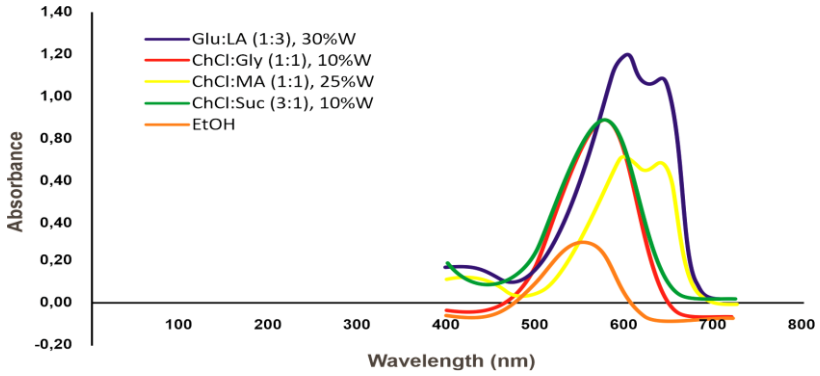



**Figure 2.** UV-Vis spectra of NR dye in NADES and ethanol.

of the studied NADES, were evaluated, and the results were presented in Table 3.

The spectral scan for the determination of NADES polarity is shown in Fig. 2, whereas the $E_{NR}$ values are reported in Table 3.

DES polarity can be determined indirectly by measuring the changes in $\lambda_{max}$ of Nile red in DES (Craveiro et al., 2016). More polar NADES shifts the $\lambda_{max}$ to a higher wavelength, and the inverse correlation in Formula 1 gives rise to lower $E_{NR}$. The NADES without added water has a polarity in the range of 45-50 kcal/mol (Dai et al., 2013). NADES investigated in our study contained different water content and had polarity in the range of 47.76-49.99 kcal mol$^{-1}$, whereas ethanol was 51.82 kcal/mol. These results indicate that ethanol was less polar compared with all NADES. The polarity of NADES is likely contributed by the number of oxygen atoms found in NADES, in particular from the -OH and -COOH moieties of NADES starting components, compared to only one -OH group in ethanol.

Various factors affect the polarity of NADES, including types of HBA: HBD components, their molar proportions, and the percentage of water added to NADES. Considering that the NADES have different HBA, stoichiometric proportions, and water percentages, their polarities could not be directly compared. However, some general characteristics can be drawn from the results.

These results indicate that NADES with organic acids had higher polarity than those observed for ChCl: Suc (3:1) and ChCl:Gly (1:1). A slight difference (1.94 kcal/mol) was observed between the most polar (ChCl:MA [1:1]) and the least polar (ChCl:Gly [1:1]) NADES. These findings are in agreement with previous data, which reported that organic acid-DES generally have the highest polarity, followed by sugar-based DES, whereas alcohol-containing DES has the least polarity (Mohd Fuad et al., 2021). Among the ChCl-based NADES used in this study, polarity arises from the difference in hydrogen bond donor ability of the HBD components. Malic acid has a stronger hydrogen bond donor ability when compared with sucrose and glycerol, thus forming stronger intermolecular forces between HBA-HBD. In addition, -OH groups existing in the molecules may function as hydrogen bond donor sites, producing highly polar NADES.

All NADES have densities that are more than 15% higher than water. NADES containing glycerol has lower density compared to NADES containing lactic acid, malic acid, and sugar, as can be seen in Table 3.

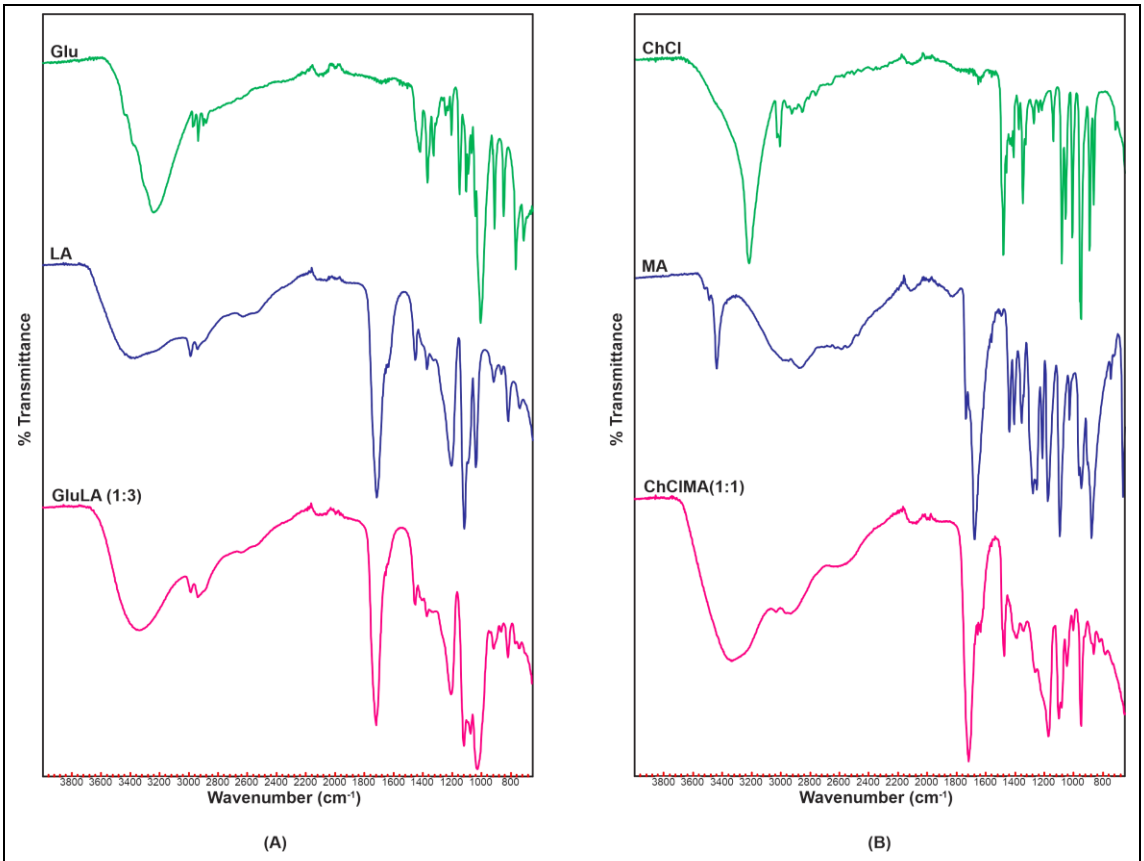



**Figure 3.** FTIR spectra of **(A)** glucose:lactic acid (Glu:LA) (1:3) system. The first, second, and third spectrum (from above) corresponds to glucose, lactic acid, and Glu:LA (1:3), respectively. **(B)** ChCl:MA (1:1) system. The first, second, and third spectra correspond to the spectra of choline chloride, malic acid, and ChCl:MA (1:1).

Viscosity is an important consideration when selecting a solvent for extraction. When NADES is used for extraction, its high viscosity can be a restrictive factor. Highly viscous liquids are difficult to disperse, which hinders efficient mass transfer. In addition, viscous liquid requires higher energy consumption for mixing or pumping in the preparation and separation steps, which leads to low extraction efficiency. However, highly viscous NADES like those observed in ChCl:Suc (3:1) may be beneficial for extraction by allowing for stable molecular interactions between NADES and the target compounds (Mitar et al., 2019)

## FTIR analysis of NADES

Analysis of the FTIR spectra of NADES and their pure components was performed to investigate chemical interactions between HBA and HBD components that synthesize deep eutectic mixtures. Results in Fig. 3 show the spectra of glu:LA (1:3) and ChCl:MA (1:1) systems, whereas Fig. 4 shows the spectra of ChCl:Gly (1:1) and ChCl:Suc (3:1) systems. In all figures, the first spectrum corresponds to the spectrum of hydrogen bond acceptor (HBA) components, the second spectrum represents HBD, and the third represents NADES.

The FTIR spectrum of glucose (Fig. 3A upper spectrum) shows a broad band at 3240 $cm^{-1}$, attributed to O-H stretching vibration. Peaks at around 2997 $cm^{-1}$ correspond to the C-H stretching. Glucose presents fingerprint bands in the region of 1420-800 $cm^{-1}$. The C-O stretching of the alcohol group appeared at 1010 $cm^{-1}$. The C-O stretching for C-O-C of the ether moiety was observed at 1153 and 1107 $cm^{-1}$.

The lactic acid spectrum is presented in Fig. 3A, the second spectrum. A broad band in the range of 3600-3150 $cm^{-1}$ is associated with the O-H stretching vibration. The C=O stretching of the carboxylic group appeared at 1718 $cm^{-1}$. The C-O stretching of hydroxyl and carboxylic acid functionalities were observed at 1207 and 1040 $cm^{-1}$. A peak at 2993 $cm^{-1}$ is assigned to the C-H stretching vibration, whereas peaks at 1457 and 1373 $cm^{-1}$ are ascribed to C-H bending of the methyl and methylene groups. The strong peak at 1120 is attributed to C-O-H bending vibration.

Choline chloride (ChCl) spectra (Figs. 3B, 4A, and 4B upper spectrum) presented a sharp band at 3218 $cm^{-1}$ corresponding to the stretching vibration of the O-H group, together with the peak at 1083 $cm^{-1}$, which corresponds to C-O stretching of the primary

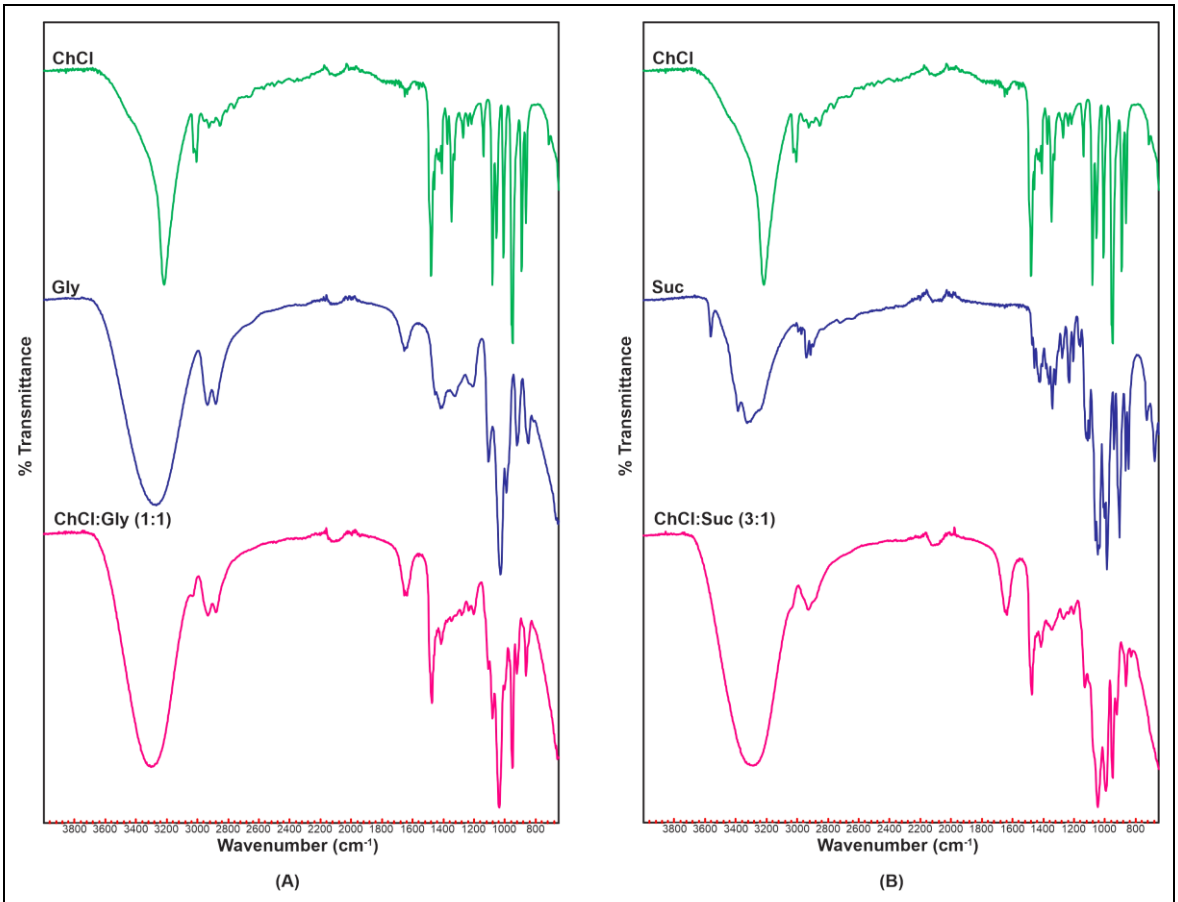



**Figure 4.** The FTIR spectra of **(A)** choline chloride:glycerol (ChCl:Gly) (1:1) system. The first, second, and third spectrum (from above) corresponds to choline chloride, glycerol, and (ChCl:Gly) (1:1), respectively. **(B)** ChCl:Suc (3:1) system. The first, second, and third spectra correspond to the spectra of choline chloride, sucrose, and ChCl:Suc (3:1).

alcohol. Peaks at 3027 and 3004 $cm^{-1}$ are ascribed to C-H stretching of -$CH_2$- and -$CH_3$, with the corresponding C-H bend vibrations at 1480 and 1349 $cm^{-1}$, respectively. The peak at 950 $cm^{-1}$ was identified to be the stretching of C-N of the quaternary ammonium compound, as reported by others (Mulia et al., 2015).

Malic acid (Fig. 3B) showed a sharp peak at 3436 $cm^{-1}$ attributed to the O-H stretching vibration. The stretching vibration C=O appeared at 1679 $cm^{-1}$. Peaks at around 1440 $cm^{-1}$ are related to the C-H bending vibration of the -CH2-. The peak at 1097 is attributed to C-O stretching vibration.

Pure glycerol presented a characteristically broad band of O-H stretching vibration of the OH groups at 3289 $cm^{-1}$ (Fig. 4A). Narrow peaks at 2939 and 2929 $cm^{-1}$ are assigned to C-H vibrations. Typical bands for glycerol were located in the ranges of 1400-800 $cm^{-1}$. The strong absorption band at 1030 $cm^{-1}$ corresponds to the vibration of two C-O linkages at C1 and C3, whereas the C-O vibration of C2 is located at 1108 $cm^{-1}$ (Guerrero et al., 2010). The vibration of the C-C skeleton was located at 997, 971, and 849 $cm^{-1}$. The peak at 1420 $cm^{-1}$ relates to the C-O-H bending vibration.

The sucrose spectrum in Fig. 4B shows a broad band with a maximum of 3328 $cm^{-1}$, which is assigned to the O-H stretching. The C-H stretching appears at 2940 and 2935 $cm^{-1}$. Similar to glucose, sucrose shows marker bands in the range of 1400-800 $cm^{-1}$. Peaks in the range of 1425-1231 $cm^{-1}$ are assigned to O-C-H, C-C-H, and C-O-H bending vibrations, as observed by others (Leopold et al., 2011). Peaks at 1121-900 $cm^{-1}$ are due to C-O and C-C stretching vibration.

To observe structural changes due to the syntheses of NADES, the FTIR spectra of NADES were compared with those of their initial components. It is apparent that all NADES spectra, Glu:LA (1:3), ChCl:MA (1:1), ChCl:Gly (1:1), and ChCl:Suc (3:1), are an overlap of the spectra of their individual components. Characteristic bands of functional groups and fingerprints were preserved. The characteristic band of the hydroxyl group appeared as broad bands in the range 3650-3100 $cm^{-1}$, which arises from O-H stretching. Also observed was the shifting of the O-H vibration stretching to a lower wave number, as seen in all NADES. The evident broadening and shifting of bands in this range is indicative of the formation of hydrogen bonds, which can stem from the hydrogen

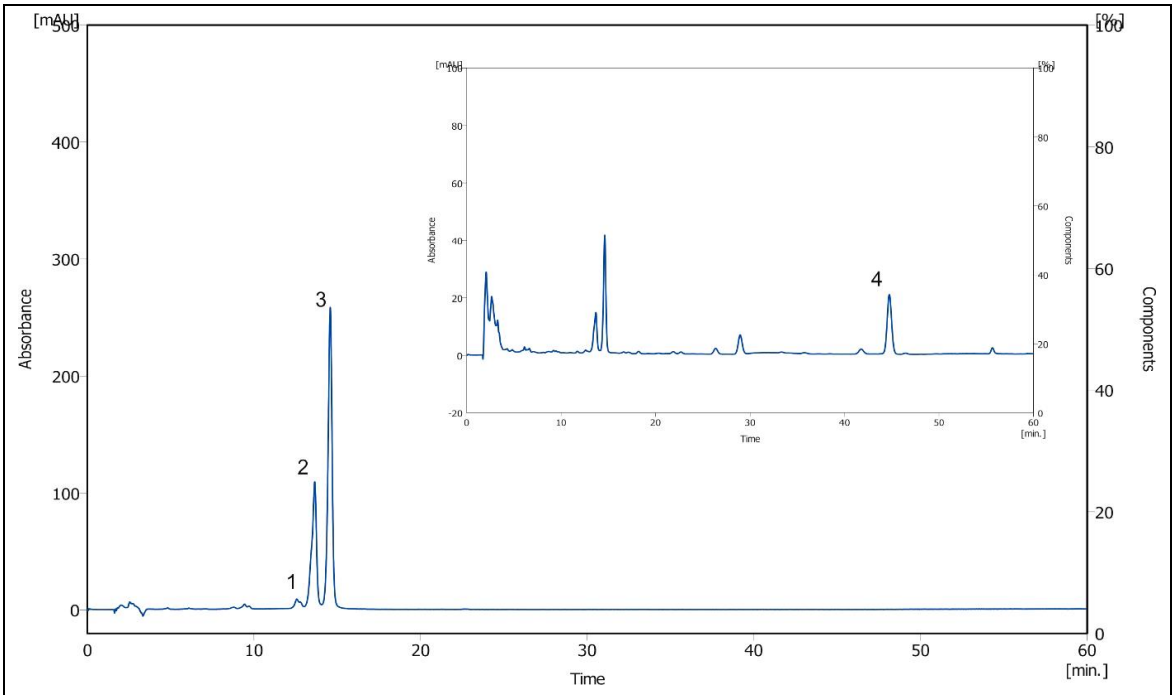



**Figure 5.** The chromatogram of Glu:LA (1:3) extract of *C. xanthorrhiza* rhizomes, showing bisdemethoxycurcumin **(1)**, demethoxycurcumin **(2)**, curcumin **(3)**, and xanthorrhizol **(4)**.

Curcuminoids and xanthorrhizol were detected at 425 and 275 nm, respectively. Inset: the chromatogram of Glu:LA (1:3) extract detected at 275 nm.

bond network formation between HBA and HBD, including with water (Jurić et al., 2021; Santana et al., 2019a). The latter was added to reduce the viscosity of NADES. Other functional groups (C-O and C=O) that can form hydrogen bonds showed observed shifting as well. The C-O group of ChCl shifted to a higher wavenumber, from 1083 to approximately 1088 $cm^{-1}$ in ChCl:MA (1:1), ChCl:Gly (1:1), and ChCl:Suc (3:1). Similarly, C=O stretching of the carboxylic group of MA shifted to a a longer wavelength (1679-1718 $cm^{-1}$). The red shift of C=O stretching has been reported to be associated with the hydrogen bond interaction between the carbonyl and hydroxyl groups (Phaechamud et al., 2016).

## Xanthorrhizol and curcuminoids analysis

Representatives of the HPLC chromatograms of NADES extract and ethanolic extract of *C. xanthorrhiza* are shown in Figs. 5 and 6, where XTZ was identified at 275 nm and BDMC, DMC, and Cur at 425 nm. The chromatograms exhibit peaks of XTZ, Cur, BDMC, and DMC, which were identified by the same retention times as reference standards. Among the four marker compounds, XTZ is the least polar, followed by Cur, BDMC and DMC, as indicated by their respective retention times.

The content of the compounds in the GluLA extract is shown in Table 4. Among solvents used to extract marker compounds, GluLA was able to extract the highest yields XTZ and curcumin. When compared to ethanol, GluLA was able to extract more than twice the amount of XTZ than ethanol. The different extraction performance among solvents reflects different affinity between the solvent and the target compounds, which can be attributed to the varying hydrogen bond formation capacity towards extracted compounds, as also indicated by their polarity (Fu et al., 2021). In addition, the viscosity (Table 2) of each NADES may influence mass transfer during extraction.

## Surface morphology study of *C. xanthorrhiza* powder

Scanning electron micrographs were analyzed to study surface morphology changes due to extraction by Glu:LA (1:3), with extraction conditions as shown in Table 1. The microscopic structure images of rhizome samples were compared with those of dried powder and ethanol extraction to understand the effect of NADES on the biomass to reveal possible extraction processes that occurred. Fig. 7 shows the surface morphology of the rhizome powder (7A1 and 7A2), rhizome extracted by Glu:LA (1:3; 7B1 and 7B2), and rhizome extracted by ethanol (7C1 and 7C2). Images were captured at 1000 and 5000 magnifications.

As seen in Figs. 7A1 and 7A2, rhizome particles without treatment show an intact, non-porous, and rela-

tively flat surfaces. This is in contrast with the case of the rhizome extracted by Glu:LA (1:3; Figs. 7B1 and 7B2). Micrograph examination at 1000× magnification revealed disintegrated and loose biomass. At 5000× magnification, the surface of rhizome material appears damaged, porous, and cracked. By comparison, in ethanol extraction, the outer surface of the rhizomes shows rough, irregular shapes. Magnification at 5000× shows porous and pits on the external structure of the particle (Figs. 7C1 and 7C2), which can be caused by erosion on the biomass surface by ethanol.

NADES have been used for the extraction of different bioactive compounds from various plant sources, including phenolic acids, flavonoids, terpenoids, saponins, anthocyanins, stilbenes, and alkaloids (Fernández et al., 2018; Mohd Fuad et al., 2021; Ruesgas-Ramón et al., 2017). Many bioactive compounds are bound in plant cell walls. Polyphenolics are synthesized in the cytoplasm and transported into the vacuoles and cell walls. Most of the macromolecules that build cell walls (cellulose, hemicellulose, pectin, and lignin) are rich in hydroxyl groups, which may interact with HBDs of NADES. Ozturk et al. (2018) showed that ChCl-based NADES effectively broke down the cell walls of orange peel in the extraction process. This allows mass transfer of plant material into NADES to dissolve bioactive compounds.

Ultrasonic-assisted extraction (UAE), when used in conjunction with DES, has been proven to increase the extraction yield of biomarkers from plant material (Ahmad et al., 2021; Hsieh et al., 2020). Most NADES

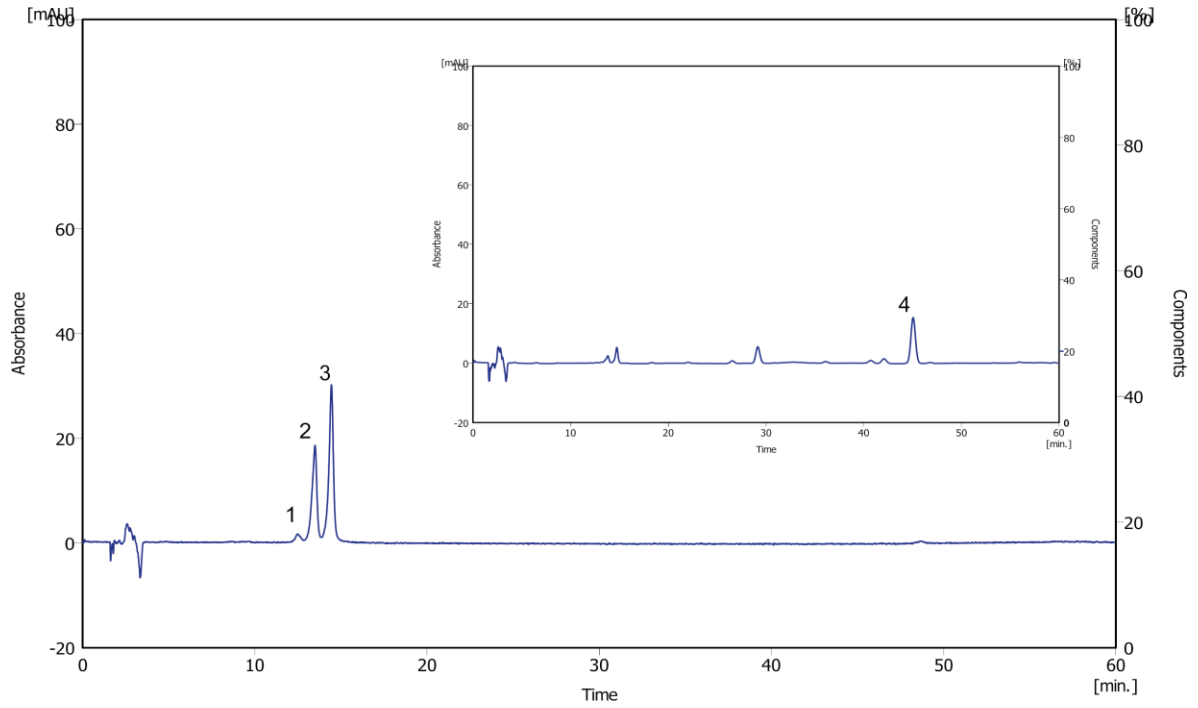



**Figure 6.** The chromatogram of ethanolic extract of *C. xanthorrhiza* rhizomes, showing bisdemethoxycurcumin **(1)**, demethoxycurcumin **(2)**, curcumin **(3)**, and xanthorrhizol **(4)**.

Curcuminoids and xanthorrhizol were detected at 425 and 275 nm, respectively. Inset: the chromatogram of ethanolic extract detected at 275 nm.

**Table 4.** The amounts of marker compounds analysed in different NADES extracts of *C. xanthorrhiza* (mg/g dried biomass ± standard deviation, n = 2).

| ***C. xanthorrhiza* extracts**[1] | **XTZ**[2] | **Cur**[2] | **BDMC**[2] | **DMC**[2] |
|---|---|---|---|---|
| Glu:LA (1:3) | $29.59 \pm 1.61^{bcde}$ | $19.57 \pm 1.63^{bde}$ | $1.35 \pm 0.43^{de}$ | $6.70 \pm 0.29^{bde}$ |
| ChCl:MA (1:1) | $7.42 \pm 0.50^{ace}$ | $7.33 \pm 0.03^{ace}$ | $0.49 \pm 0.001$ | $3.17 \pm 0.03^{ace}$ |
| ChCl:Gly (1:1) | $19.68 \pm 1.54^{abde}$ | $20.83 \pm 3.24^{abde}$ | $1.20 \pm 0.22$ | $6.29 \pm 1.23^{bde}$ |
| ChCl:Suc (3:1) | $6.14 \pm 0.06^{ace}$ | $8.52 \pm 0.12^{ac}$ | $0.70 \pm 0.04$ | $3.13 \pm 0.11^{ace}$ |
| Ethanol | $11.38 \pm 0.04^{abcd}$ | $1.38 \pm 0.01^{ac}$ | $0.24 \pm 0.06$ | $0.71 \pm 0.03^{abcd}$ |

[1]Glu:LA (glucose:lactic acid), ChCl:MA (choline chloride:malic acid), ChCl:Gly (choline chloride:glycerol), and ChCl:Suc (choline chloride:sucrose). [2]XTZ (xanthorrhizol), Cur (curcumin), BDMC (bisdemethoxycurcumin), and DMC (demethoxycurcumin). Data are expressed as mean ± SD (n = 2). Different letters indicate statistically significant differences with Tukey analysis ($p<0.05$).

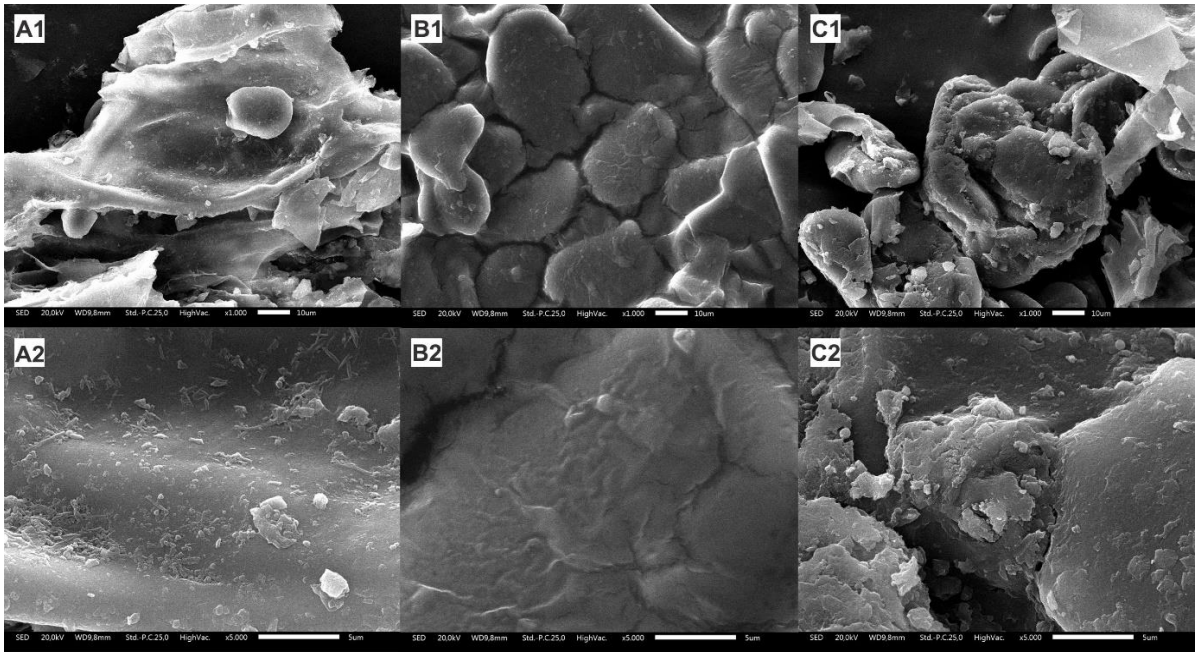



**Figure 7.** Scanning electron micrographs of *C. xanthorrhiza* rhizome powder **(A1, A2)**, rhizome powder extracted by Glu:LA (1:3) combined with sonication **(B1, B2)**, and rhizome powder extracted by ethanol **(C1, C2)**.
Each sample was captured at 1000 and 5000× magnification.

share similar characteristics of having high viscosity and low vapor pressure. As with other solvent systems, ultrasonic waves induce mechanical vibrations when applied to GluLA (1:3), which propagates into cavitation bubbles. However, due to the high viscosity of DES, the application of UAE requires a high-intensity ultrasound to initiate mechanical vibration. The low vapor pressure characteristic of DES is beneficial for DES-UAE, as DES would incite more intense bubble collapse than conventional solvents (Wen et al., 2018). The implosion of the cavitation bubbles creates high shear force, which is mainly responsible for the disintegration and detexturation of raw materials (Chemat et al., 2017), as also observed in the present study. The disruption of surface structure by Glu:LA-UAE, as evidenced by the loosening and cracking of the outer surface of the rhizome (Fig. 4C-D), would increase the penetration of Glu:LA into the intracellular structure. This effect, combined with the affinity of Glu:LA (1:3) to marker compounds, facilitates the mass transfer of the biomarkers from the cell matrix toward bulk Glu:LA. All the tested NADES showed radical scavenging activity on the DPPH radicals. This effect might be beneficial to reduce oxidative damage on the targeted biomarkers, which is caused by OH• radicals propagated via ultrasonic cavitation (Vilkhu et al., 2008).

Although morphological examination of the ethanol extraction revealed a damaged surface, this result was obtained after a prolonged period of extraction (24 h), compared to that of 20 min ultrasonication assisted NADES extraction. Moreover, Glu:LA obtained higher yields of XTZ and curcuminoids compared with ethanol extraction. Glu:LA (1:3) combined with UAE may be of interest toward the development of a more efficient extraction process to obtain a higher yield of XTZ and curcuminoids.

## Antioxidant activities of NADES and NADES extracts

In this study, FRAP and DPPH assays were applied to evaluate the antioxidant capacity of NADES and NADES extracts. FRAP assay estimates the reducing capability of antioxidant compounds based upon a single electron transfer (SET) from antioxidant compounds to reduce Fe(III) – TPTZ into the blue-colored Fe(II) – TPTZ under acidic conditions. DPPH assay measures antioxidant activity based on radical scavenging activity through mixed mechanisms of hydrogen atom transfer and SET. FRAP and DPPH assays have been widely used for the evaluation of antioxidant activity in botanicals and biological samples due to their robustness, sensitivity, and low cost (Prior et al., 2005). Although the antioxidant activity of NADES has been poorly studied, some studies have discussed this phenomenon (Hayyan et al., 2015; Radošević et al., 2016).

Results in Table 5 show that in both assays, all pure NADES showed antioxidant activities. ChCl:MA (1:1) gave the highest reducing ability (181.65 µmol TE gram$^{-1}$ NADES), followed by ChCl: Suc (3:1) and ChCl: Gly (1:1), whereas Glu:LA (1:3) showed the

**Table 5.** Antioxidant activities of NADES and NADES extracts.

| Sample name | FRAP (µmol TE/g NADES or solvent)* | DPPH (µmol AAE/g NADES or solvent)† | FRAP (mmol TE/g NADES extract) | DPPH (µmol AAE/g NADES extract) |
|---|---|---|---|---|
| Glu:LA (1:3) | 41.22 ± 0.27 $^{bcde}$ | 0.25 ± 0.005 $^{bcde}$ | 2.75 ± 0.06 $^{bcde}$ | 5.37 ± 0.04 $^{bcde}$ |
| ChCl:MA (1:1) | 181.65 ± 1.37 $^{acde}$ | 0.44 ± 0.001 $^{acde}$ | 1.46 ± 0.03 $^{acde}$ | 1.96 ± 0.01 $^{acde}$ |
| ChCl:Gly (1:1) | 60.47 ± 0.24 $^{abd}$ | 0.18 ± 0.005 $^{abde}$ | 1.72 ± 0.02 $^{abde}$ | 2.41 ± 0.14 $^{abde}$ |
| ChCl:Suc (3:1) | 137.29 ± 0.57 $^{abce}$ | 0.20 ± 0.002 $^{abce}$ | 0.89 ± 0.02 $^{abce}$ | 0.93 ± 0.06 $^{abce}$ |
| Ethanol | 57.48 ± 1.25 $^{abd}$ | 0.03 ± 0.001 $^{abcd}$ | 2.92 ± 0.07 $^{abcd}$ | 0.39 ± 0.03 $^{abcd}$ |

Data are expressed as mean ± SD (n = 4). Different letters indicate statistically significant differences with Tukey analysis ($p<0.05$). *µmol TE (Trolox equivalent)/g. †µmol AAE (ascorbic acid equivalent)/g.

lowest ability to transfer electron, indicating that NADES can contribute to the electron and hydrogen atom donating ability. The high reducing capacity of ChCl:MA (1:1) is likely attributable to the malic acid component in this NADES system. The FRAP activity is three times higher than its corresponding glycerol-based NADES, ChCl: Gly (1:1), since alcohol is a poorer electron donor than acid. Regarding the DPPH assay, all NADES showed radical scavenging activity that was higher than ethanol, suggesting that NADES can contribute to the scavenging activity. Similarly, as in the FRAP assay, Glu:LA (1:3) showed the lowest activity compared to other NADES. Although lactic acid is known in the literature to have strong antioxidant activity, the presence of glucose as a hydrogen bond donor-acceptor appears to weaken the electron-donating ability or hydrogen atom transfer of lactic acid.

FRAP and DPPH activities of NADES and ethanol extracts were higher than the NADES systems. In the FRAP assay, ethanol extract showed the highest value compared to NADES extracts. Previous studies have identified various phytocompounds in the ethanol extract of *C. xanthorrhiza* rhizomes (Klau et al., 2023), including flavonoids, alkaloids, and terpenes, all of which may contribute to the antioxidant activities of the extracts. Different results were obtained by DPPH assay. All the tested NADES extracts exhibited higher antioxidant activity than ethanol extract. NADES may stabilize antioxidant compounds by intermolecular interaction through hydrogen bond formation, as reported previously (Barbieri et al., 2020). Among the studied NADES extracts, Glu:LA (1:3) extract gave the highest activity, followed by ChCl: Gly (1:1) > ChCl:MA (1:1) > ChCl: Suc (3:1) extracts. These results might be due to the amount of marker compounds obtained in each NADES (Table 4) or the kinds of compounds extracted by the solvents.

## Toxicity of NADES and NADES extracts

DES is considered harmless and eco-friendly because most of its individual components can be found in nature and are generally safe (Abbott et al., 2004). However, recent studies have reported that the non-toxic behavior of individual DES components can differ from the corresponding DES mixture (Hayyan et al., 2013). Therefore, assessment of the biological toxicity of NADES is essential. Limited studies reported the toxicity evaluation of NADES using a variety of organisms such as vertebrates, invertebrates, plants, microorganisms, and cell lines (Hayyan et al., 2015; Juneidi et al., 2016). In this study, toxicity profiles of NADES and NADES extracts were assayed using *E. coli* as a model organism. This bacterium is one of the most common microorganisms that has been used widely for testing chemical toxicity (Hayyan et al., 2013).

Fig. 8 shows *E. coli* growth curves in the presence of different NADES or NADES extracts or ethanol extract. Control (red line) in which no NADES or extracts were added exhibited the expected growth pattern. The lag phase (less than 1 h) was observed, in which the growth stayed approximately the same due to the adaptation of the bacterium to the new environment. This was then followed by an exponential growth phase (log phase), where it reached maximum growth to an OD of around 0.6 within 1 h. Thereafter, the growth rate decreased to enter a stationary phase, where the maximum OD of around 1.2 was observed after 15 h of incubation.

A similar growth profile was observed for culture media that was supplemented by Glu:LA (1:3), ChCl:Gly (1:1), and ChCl:Suc (3:1), indicating no inhibition on *E. coli* growth, thus non-toxicity of these NADES to *E. coli*. In contrast, the addition of ChCl:MA (1:1) to the cultured media resulted in very low OD over time. Unlike ChCl:Gly (1:1) and ChCl:Suc (3:1), ChCl:MA (1:1) inhibited the growth of

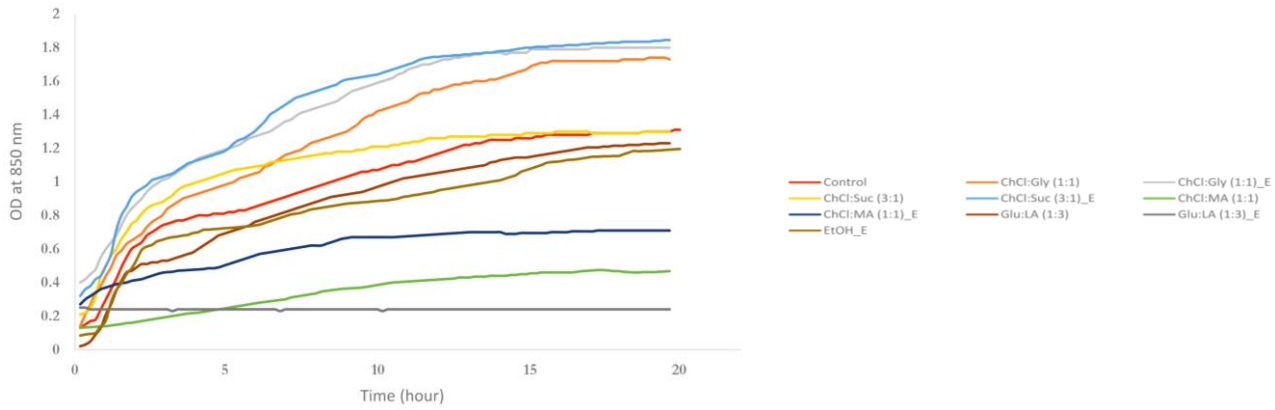



**Figure 8.** Growth curves of *E. coli* in the presence of NADES or their respective extract or ethanol extract of *C. xanthorrhiza* (50 µL).
The cells were grown in LB media supplemented by these samples, and the OD was read at 850 nm continuously every 15 min for over 20 h. Letter E indicates extracts.

the bacterium. The HBD component (malic acid) plays a role in the toxicity of ChCl:MA (1:1). Various studies have reported that choline chloride-based DES with organic acids, as HBDs are generally toxic toward microorganisms (Yang, 2019), which can be due to pH decreases. A study by de Morais et al. (2015) found that toxicity of acid-containing NADES may be due to the interaction between NADES and the cellular membrane. This finding explains the higher toxicity of DES with the increasing lipophilicity of the organic acid components. Previously, choline chloride based-DES with organic acids such as ascorbic acid, lactic acid, glycolic acid, and citric acid as HBD were reported to inhibit the growth of *Vibrio fischeri*, a Gram-negative marine bacterium (Lomba et al., 2021). The degree of toxicity of the acid-containing DES is likely associated with the lipophilicity of the organic acids that enable it to cross the cell membrane, giving rise to disruption of the cell membrane. It should be noted, however, that a different result was obtained for Glu:LA (1:3). Unlike ChCl:MA (1:1), Glu:LA (1:3) did not exhibit inhibitions on *E. coli*, which may be due to the higher pH of Glu:LA (1:3) compared to ChCl:MA (1:1), as shown in Table 3.

In the cases of ChCl:Gly (1:1), ChCl:Suc (3:1), and ChCl:MA (1:1), similar growth patterns were observed with their respective NADES extracts. *C. xanthorrhiza* extracts of ChCl:Gly (1:1) and ChCl:Suc (3:1) did not pose toxicity to *E. coli*, as can be seen by the growth curves. In a similar pattern, *C. xanthorrhiza* extracted by ChCl:MA (1:1) showed inhibition in the bacterial growth, similar to ChCl:MA (1:1). Interestingly, unlike Glu:LA (1:3), the extract using Glu:LA (1:3) inhibited the bacterium. These results may suggest that phytocompounds extracted by Glu:LA (1:3) produce synergistic antibacterial activity that reduces the bacterium viability. However, the ethanolic extract of *C. xanthorrhiza* was not toxic to *E. coli*. As indicated in Table 4, different amounts of XTZ and curcuminoids (CURS) were extracted using various NADES and ethanol. In addition to XTZ and CURS, other phytocompounds extracted by these solvents are also likely to contribute to the difference in bacterial toxicity profiles.

Recent studies have reported the use of other bacteria to evaluate the toxicity of DES (Hayyan et al., 2013). The use of bacteria in bioassay toxicity tests provides some benefits such as a short life cycle, easy, and relatively inexpensive (Hassan et al., 2016). In this study, the bacterial inhibition method was assayed by real-time monitoring of bacterial growth. Continuous observation of the growth over time reflects real interaction between NADES and the bacteria, thus yielding more reliable results than other inhibition methods, such as the disk diffusion test. In addition, the use of liquid media overcomes the limitations of NADES—i.e., high viscosity and density, which limits the diffusion of NADES in the disk.

## CONCLUSION

Glu:LA (1:3), ChCl:MA (1:1), ChCl:Gly (1:1), and ChCl:Suc (3:1) were studied for their extraction on XTZ and curcuminoids from *C. xanthorrhiza*. This study reveals the basic physicochemical properties of the studied NADES. All NADES were characterized by high density and viscosity. Different polarities were observed, with NADES containing organic acids showing higher polarity compared to those without acid components. All the tested NADES systems showed antioxidative activity by DPPH radical scavenging activity and Fe(II) reducing capacity. Pure NADES have also displayed no toxicity towards *E. coli*, except for ChCl: MA (1:1). FTIR results confirmed the formation of hydrogen bonds between NADES components. Simultaneous determination of the marker compounds by HPLC found that when compared with ethanol and other NADES, Glu:LA (1:3) obtained the highest content of XTZ. This result suggests the potential of using Glu:LA (1:3) to replace

ethanol and still obtain good marker content. Surface morphology analysis evidenced the effect of the combined use of NADES and ultrasonication for extraction, as demonstrated by the disintegration and the loosening of the rhizome powder. The present study found that NADES extracts of Glu:LA (1:3) and ChCl:MA (1:1) showed toxicity on *E. coli*, as seen by their inhibition of bacterium growth. This finding recommends the pH modification of Glu:LA extract before further applications.

## CONFLICT OF INTEREST

The authors declare no conflicts of interest.

## ACKNOWLEDGMENTS

The authors would like to thank the Directorate of Research and Development (Direktorat Riset dan Pengembangan), Universitas Indonesia, for publication funding support through PUTI Pascasarjana grant (NKB-068/UN2.RST/ HKP.05.00/2022); the Ministry of Research and Technology and Higher Education of the Republic of Indonesia for PKN/PK 2023 (Grant number: NKB-1084/UN2.RST/ HKP.05.00/2023); and Badan Riset and Inovasi Nasional through the National Metabolomics Collaborative Research Center (research grant for the year 2023).

## REFERENCES

Abbott AP, Boothby D, Capper G, Davies DL, Rasheed RK (2004) Deep eutectic solvents formed between choline chloride and carboxylic acids: versatile alternatives to ionic liquids. J Am Chem Soc 126: 9142–9147. https://doi.org/10.1021/ja048266j

Ahmad I, Arifianti AE, Sakti AS, Saputri FC, Mun'im A (2020) Simultaneous natural deep eutectic solvent-based ultrasonic-assisted extraction of bioactive compounds of cinnamon bark and sappan wood as a dipeptidyl peptidase IV Inhibitor. Molecules 25: 3832–3842. https://doi.org/10.3390/molecules25173832

Ahmad I, Syakfanaya AM, Azminah A, Saputri FC, Mun'im A (2021) Optimization of betaine-sorbitol natural deep eutectic solvent-based ultrasound-assisted extraction and pancreatic lipase inhibitory activity of chlorogenic acid and caffeine content from robusta green coffee beans. Heliyon 7: E07702. https://doi.org/10.1016/j.heliyon.2021.e07702

Amartya AS (2022) The use of choline chloride sugar based-natural deep eutectic solvents for extraction of *Curcuma xanthorrhiza* Roxb. rhyzomes with ultrasound assisted-extraction. (Bachelor degree), Universitas Indonesia, Depok.

AOAC (2012) Official Methods of Analysis: Guidelines for Dietary Supplements and Botanical. Washington DC: Association of Official Analytical Chemists.

Bakirtzi C, Triantafyllidou K, Makris DP (2016) Novel lactic acid-based natural deep eutectic solvents: Efficiency in the ultrasound-assisted extraction of antioxidant polyphenols from common native Greek medicinal plants. J Appl Res Med Aromat Plants 3: 120–127. https://doi.org/10.1016/j.jarmap.2016.03.003

Barbieri JB, Goltz C, Batistão Cavalheiro F, Theodoro Toci A, Igarashi-Mafra L, Mafra MR (2020) Deep eutectic solvents applied in the extraction and stabilization of rosemary (*Rosmarinus officinalis* L.) phenolic compounds. Ind Crops Prod 144: 112049. https://doi.org/10.1016/j.indcrop.2019.112049

Bolanos de la Torre AAS, Henderson T, Nigam PS, Owusu-Apenten RK (2015) A Universally calibrated microplate ferric reducing antioxidant power (FRAP) assay for foods and applications to Manuka honey. Food Chem 174: 119–123. https://doi.org/10.1016/j.foodchem.2014.11.009

Chemat F, Rombaut N, Sicaire A-G, Meullemiestre A, Fabiano-Tixier A-S, Abert-Vian M (2017) Ultrasound assisted extraction of food and natural products. Mechanisms, techniques, combinations, protocols and applications. A review. Ultrason Sonochem 34: 540–560. https://doi.org/10.1016/j.ultsonch.2016.06.035

Craveiro R, Aroso I, Flammia V, Carvalho T, Viciosa MT, Dionísio M, Barreiros S, Reis RL, Duarte ARC, Paiva A (2016) Properties and thermal behavior of natural deep eutectic solvents. J Mol Liq 215: 534–540. https://doi.org/10.1016/j.molliq.2016.01.038

Dai Y, van Spronsen J, Witkamp GJ, Verpoorte R, Choi YH (2013) Natural deep eutectic solvents as new potential media for green technology. Anal Chim Acta 766: 61–68. https://doi.org/10.1016/j.aca.2012.12.019

de Morais P, Gonçalves F, Coutinho JAP, Ventura SPM (2015) Ecotoxicity of cholinium-based deep eutectic solvents. ACS Sustain Chem Eng 3: 3398–3404. https://doi.org/10.1021/acssuschemeng.5b01124

Devaraj S, Esfahani AS, Ismail S, Ramanathan S, Yam MF (2010) Evaluation of the antinociceptive activity and acute oral toxicity of standardized ethanolic extract of the rhizome of *Curcuma xanthorrhiza* Roxb. Molecules 15: 2925–2934. https://doi.org/10.3390/molecules15042925

Devaraj S, Ismail S, Ramanathan S, Yam MF (2014) Investigation of antioxidant and hepatoprotective activity of standardized *Curcuma xanthorrhiza* rhizome in carbon tetrachloride-induced hepatic damaged rats. Sci World J 2014: 353128. https://doi.org/10.1155/2014/353128

Duan L, Dou L-L, Guo L, Li P, Liu EH (2016) Comprehensive evaluation of deep eutectic solvents in extraction of bioactive natural products. ACS Sustain Chem Eng 4: 2405-2411. https://doi.org/10.1021/acssuschemeng.6b00091

Erpina E, Rafi M, Darusman LK, Vitasari A, Putra BR, Rohaeti E (2017) Simultaneous quantification of curcuminoids and xanthorrhizol in *Curcuma xanthorrhiza* by high-performance liquid chromatography. J Liq Chromatogr Rel Technol 40: 635–639. https://doi.org/10.1080/10826076.2017.1343729

Fernández MdlÁ, Boiteux J, Espino M, Gomez FJV, Silva MF (2018) Natural deep eutectic solvents-mediated extractions: The way forward for sustainable analytical developments. Anal Chim Acta 1038: 1–10. https://doi.org/10.1016/j.aca.2018.07.059

Fu X, Wang D, Belwal T, Xie J, Xu Y, Li L, Zou L, Zhang L, Luo Z (2021) Natural deep eutectic solvent enhanced pulse-ultrasonication assisted extraction as a multi-stability protective and efficient green strategy to extract anthocyanin from blueberry pomace. LWT 144: 111220. https://doi.org/10.1016/j.lwt.2021.111220

Grozdanova T, Trusheva B, Alipieva K, Popova M, Dimitrova L, Najdenski H, Zaharieva MM, Ilieva Y, Vasileva B, Miloshev G, Georgieva M, Bankova V (2020) Extracts of medicinal plants with natural deep eutectic solvents: enhanced antimicrobial activity and low genotoxicity. BMC Chemistry 14: 73. https://doi.org/10.1186/s13065-020-00726-x

Guerrero P, Retegi A, Gabilondo N, de la Caba K (2010) Mechanical and thermal properties of soy protein films processed by casting and compression. J Food Eng 100: 145–151. https://doi.org/10.1016/j.jfoodeng.2010.03.039

Hassan SHA, Van Ginkel SW, Hussein MAM, Abskharon R, Oh S-E (2016) Toxicity assessment using different bioassays and microbial biosensors. Environ Int 92-93: 106–118. https://doi.org/10.1016/j.envint.2016.03.003

Hayyan M, Hashim MA, Hayyan A, Al-Saadi MA, AlNashef IM, Mirghani MES, Saheed OK (2013) Are deep eutectic solvents benign or toxic? Chemosphere 90: 2193–2195. https://doi.org/10.1016/j.chemosphere.2012.11.004

Hayyan M, Looi CY, Hayyan A, Wong WF, Hashim MA (2015) *In vitro* and *in vivo* toxicity profiling of ammonium-based deep eutectic solvents. PLoS One 10: e0117934. https://doi.org/10.1371/journal.pone.0117934

He Y, Yue Y, Zheng X, Zhang K, Chen S, Du ZJM (2015) Curcumin, inflammation, and chronic diseases: How are they linked? Molecules 20: 9183–9213. https://doi.org/10.3390/molecules20059183

Hilma R, Wulandari ETS, Arman Z (2020) Fruit stalk extract from chili peppers (*Capsicum annum* L.) as a natural antioxidant to inhibit oxidation in crude palm oil. J Kim Sains Apl 23: 124–128. https://doi.org/10.14710/jksa.23.4.124-128

Hirschhorn HH (1983) Botanical remedies of the former Dutch East Indies (Indonesia). Part I: Eumycetes, pteridophyta, gymnospermae, angiospermae (monocotyledones only). J Ethnopharmacol 7: 123–156. https://doi.org/10.1016/0378-8741(83)90016-8

Hsieh Y-H, Li Y, Pan Z, Chen Z, Lu J, Yuan J, Zhu Z, Zhang J (2020) Ultrasonication-assisted synthesis of alcohol-based deep eutectic solvents for extraction of active compounds from ginger. Ultrason Sonochem 63: 104915. https://doi.org/10.1016/j.ultsonch.2019.104915

Hwang JK, Shim JS, Pyun YR (2000) Antibacterial activity of xanthorrhizol from *Curcuma xanthorrhiza* against oral pathogens. Fitoterapia 71: 321-323. https://doi.org/10.1016/S0367-326X(99)00170-7

Juneidi I, Hayyan M, Mohd Ali O (2016) Toxicity profile of choline chloride-based deep eutectic solvents for fungi and *Cyprinus carpio* fish. Environ Sci Pollut Res 23: 7648–7659. https://doi.org/10.1007/s11356-015-6003-4

Jurić T, Uka D, Holló BB, Jović B, Kordić B, Popović BM (2021) Comprehensive physicochemical evaluation of choline chloride-based natural deep eutectic solvents. J Mol Liq 343: 116968. https://doi.org/10.1016/j.molliq.2021.116968

Kementerian Kesehatan RI (2017) Farmakope Herbal Indonesia (2ed.). Jakarta: Kementerian Kesehatan Republik Indoensia.

Klau ME, Rohaeti E, Rafi M, Artika IM, Ambarsari L, Nurcholis W (2023) Metabolite profiling of *Curcuma xanthorriza* varieties grown in different regions using UHPLC-Q-Orbitrap-HRMS and chemometrics analysis. Biointerface Res Appl Chem 13: 26. https://doi.org/10.33263/BRIAC131.026

Kusumowardhani ASP (2022) Extraction of Javanese turmeric rhizomes (*Curcuma xanthorrhiza* Roxb) with natural deep eutectic solvents based on choline chloride with sugar alcohol using ultrasound assisted-extraction. (Bachelor degree), Universitas Indonesia, Depok.

Leopold LF, Leopold N, Diehl H-A, Socaciu C (2011) Quantification of carbohydrates in fruit juices using FTIR spectroscopy and multivariate analysis. Spectroscopy 26: 285890. https://doi.org/10.3233/SPE-2011-0529

Liu Y, Li J, Fu R, Zhang L, Wang D, Wang S (2019) Enhanced extraction of natural pigments from *Curcuma longa* L. using natural deep eutectic solvents. Ind Crops Prod 140: 111620. https://doi.org/10.1016/j.indcrop.2019.111620

Lomba L, Ribate M, Sangüesa E, Concha J, Garralaga M, Errazquin D, García CB, Giner B (2021) Deep eutectic solvents: Are they safe? Appl Sci 11: 10061. https://doi.org/10.3390/app112110061

Mary HPA, Susheela GK, Jayasree S, Nizzy AM, Rajagopal B, Jeeva S (2012) Phytochemical characterization and antimicrobial activity of *Curcuma xanthorrhiza* Roxb. Asian Pac J Trop Biomed 2: S637–S640. https://doi.org/10.1016/S2221-1691(12)60288-3

Mitar A, Panić M, Prlić Kardum J, Halambek J, Sander A, Zagajski Kučan K, Radojčić Redovniković I, Radošević K (2019) Physicochemical properties, cytotoxicity, and antioxidative activity of natural deep eutectic solvents containing organic acid. Chem Biochem Eng Q 33: 1–18. https://doi.org/10.15255/CABEQ.2018.1454

Mohd Fuad F, Mohd Nadzir M, Harun Kamaruddin A (2021) Hydrophilic natural deep eutectic solvent: A review on physicochemical properties and extractability of bioactive compounds. J Mol Liq 339: 116923. https://doi.org/10.1016/j.molliq.2021.116923

Mulia K, Krisanti E, Terahadi F, Putri S (2015) Selected natural deep eutectic solvents for the extraction of a-mangostin from mangosteen (*Garcinia mangostana* L.) pericarp. Int J Technol 6: 1211-1220. https://doi.org/10.14716/ijtech.v6i7.1984

Nadia B (2022) Extraction of Javanese turmeric rhizomes (*Curcuma xanthorrhiza* Roxb) with choline chloride and organic acid-based natural deep eutectic solvents by ultrasound assisted-extraction. (Bachelor degree), Universitas Indonesia, Depok.

Nurcholis W, Munshif AA, Ambarsari L (2018) Xanthorrhizol contents, α-glucosidase inhibition, and cytotoxic activities in ethyl acetate fraction of *Curcuma zanthorrhiza* accessions from Indonesia. Rev Bras Farmacogn 28: 44–49. https://doi.org/10.1016/j.bjp.2017.11.001

Ogihara W, Aoyama T, Ohno H (2004) Polarity measurement for ionic liquids containing dissociable protons. Chem Lett 33: 1414-1415. https://doi.org/10.1246/cl.2004.1414

Oktaviyanti ND, Kartini, Mun'im A (2019) Application and optimization of ultrasound-assisted deep eutectic solvent for the extraction of new skin-lightening cosmetic materials from *Ixora javanica* flower. Heliyon 5: e02950. https://doi.org/10.1016/j.heliyon.2019.e02950

Oon SF, Nallappan M, Tee TT, Shohaimi S, Kassim NK, Sa'ariwijaya MSF, Cheah YH (2015) Xanthorrhizol: A review of its pharmacological activities and anticancer properties. Cancer Cell Int 15: 100. https://doi.org/10.1186/s12935-015-0255-4

Ozturk B, Parkinson C, Gonzalez-Miquel M (2018) Extraction of polyphenolic antioxidants from orange peel waste using deep eutectic solvents. Sep Purif Methods 206: 1–13. https://doi.org/10.1016/j.seppur.2018.05.052

Patil SS, Pathak A, Rathod VK (2021) Optimization and kinetic study of ultrasound assisted deep eutectic solvent based extraction: a greener route for extraction of curcuminoids from *Curcuma longa*. Ultrason Sonochem 70: 105267. https://doi.org/10.1016/j.ultsonch.2020.105267

Phaechamud T, Tuntarawongsa S, Charoensuksai P (2016) Evaporation behavior and characterization of eutectic solvent and ibuprofen eutectic solution. AAPS PharmSciTech 17: 1213–1220. https://doi.org/10.1208/s12249-015-0459-x

Prior RL, Wu X, Schaich K (2005) Standardized methods for the determination of antioxidant capacity and phenolics in foods and dietary supplements. J Agric Food Chem 53: 4290–4302. https://doi.org/10.1021/jf0502698

Putri CR (2022) Optimization of glucose-organic acid-based natural deep eutectic solvents and ultrasound-assisted extraction of *Curcuma xanthorrhiza* Roxb rhizomes [Indonesian]. (Bachelor degree), Universitas Indonesia, Depok.

Radošević K, Ćurko N, Gaurina Srček V, Cvjetko Bubalo M, Tomašević M, Kovačević Ganić K, Radojčić Redovniković I (2016) Natural deep eutectic solvents as beneficial extractants

for enhancement of plant extracts bioactivity. LWT-Food Sci Technol 73: 45–51. https://doi.org/10.1016/j.lwt.2016.05.037

Radošević K, Cvjetko Bubalo M, Gaurina Srček V, Grgas D, Landeka Dragičević T, Radojčić Redovniković I (2015) Evaluation of toxicity and biodegradability of choline chloride based deep eutectic solvents. Ecotoxicol Environ Safe 112: 46–53. https://doi.org/10.1016/j.ecoenv.2014.09.034

Reichardt C (1994) Solvatochromic dyes as solvent polarity indicators. Chem Rev 94: 2319–2358. https://doi.org/10.1021/cr00032a005

Rente D, Paiva A, Duarte AR (2021) The role of hydrogen bond donor on the extraction of phenolic compounds from natural matrices using deep eutectic systems. Molecules 26: 2336. https://doi.org/10.3390/molecules26082336

Ruesgas-Ramón M, Figueroa-Espinoza MC, Durand E (2017) Application of deep eutectic solvents (DES) for phenolic compounds extraction: overview, challenges, and opportunities. J Agric Food Chem 65: 3591–3601. https://doi.org/10.1021/acs.jafc.7b01054

Sahebkar A, Serban M-C, Ursoniu S, Banach M (2015) Effect of curcuminoids on oxidative stress: A systematic review and meta-analysis of randomized controlled trials. J Funct Foods 18: 898–909. https://doi.org/10.1016/j.jff.2015.01.005

Santana APR, Andrade DF, Mora-Vargas JA, Amaral CDB, Oliveira A, Gonzalez MH (2019a) Natural deep eutectic solvents for sample preparation prior to elemental analysis by plasma-based techniques. Talanta 199: 361–369. https://doi.org/10.1016/j.talanta.2019.02.083

Santana APR, Mora-Vargas JA, Guimarães TGS, Amaral CDB, Oliveira A, Gonzalez MH (2019b) Sustainable synthesis of natural deep eutectic solvents (NADES) by different methods. J Mol Liq 293: 111452. https://doi.org/10.1016/j.molliq.2019.111452

Simamora A, Timotius KH, Yerer MB, Setiawan H, Mun'im A (2022) Xanthorrhizol, a potential anticancer agent, from *Curcuma xanthorrhiza* Roxb. Phytomedicine 105: 154359. https://doi.org/10.1016/j.phymed.2022.154359

Torregrosa-Crespo J, Marset X, Guillena G, Ramón DJ, María Martínez-Espinosa R (2020) New guidelines for testing "Deep eutectic solvents" toxicity and their effects on the environment and living beings. Sci Total Environ 704: 135382. https://doi.org/10.1016/j.scitotenv.2019.135382

Vilkhu K, Mawson R, Simons L, Bates D (2008) Applications and opportunities for ultrasound assisted extraction in the food industry — A review. Innov Food Sci Emerg Technol 9: 161–169. https://doi.org/10.1016/j.ifset.2007.04.014

Wen C, Zhang J, Zhang H, Dzah CS, Zandile M, Duan Y, Ma H, Luo X (2018) Advances in ultrasound assisted extraction of bioactive compounds from cash crops – A review. Ultrason Sonochem 48: 538–549. https://doi.org/10.1016/j.ultsonch.2018.07.018

Yang Z (2019) Toxicity and biodegradability of deep eutectic solvents and natural deep eutectic solvents. In: Ramón DJ. Guillena G (Eds.), Deep Eutectic Solvents. New Jersey: Wiley-VCH pp 43–60. https://doi.org/10.1002/9783527818488.ch3

**AUTHOR CONTRIBUTION:**

| Contribution | Simamora A | Timotius KH | Setiawan H | Putra MY | Mun'im A |
|---|---|---|---|---|---|
| Concepts or ideas | x | x | x | x | x |
| Design | x | x | | | x |
| Definition of intellectual content | x | x | x | x | x |
| Literature search | x | x | | | x |
| Experimental studies | x | x | | | x |
| Data acquisition | x | | | | |
| Data analysis | x | x | | | x |
| Statistical analysis | x | | | | |
| Manuscript preparation | x | x | x | x | x |
| Manuscript editing | x | x | x | x | x |
| Manuscript review | x | x | x | x | x |

**Citation Format:** Simamora A, Timotius KH, Setiawan H, Putra MY, Mun'im A (2023) Natural deep eutectic solvent extraction of xanthorrhizol and curcuminoids from *Curcuma xanthorrhiza* Roxb and simultaneous determination by high-performance liquid chromatography. J Pharm Pharmacogn Res 11(6): 1056–1071. https://doi.org/10.56499/jppres23.1727_11.6.1056

**Publisher's Note:** All claims expressed in this article are solely those of the authors and do not necessarily represent those of their affiliated organizations, or those of the publisher, the editors and the reviewers. Any product that may be evaluated in this article, or claim that may be made by its manufacturer, is not guaranteed or endorsed by the publisher.

**Open Access:** This article is distributed under the terms of the Creative Commons Attribution 4.0 International License (http://creativecommons.org/ licenses/by/4.0/), which permits use, duplication, adaptation, distribution and reproduction in any medium or format, as long as you give appropriate credit to the original author(s) and the source, provide a link to the Creative Commons license and indicate if changes were made.